

DeMarking: A Defense for Network Flow Watermarking in Real-Time

Yali Yuan
Southeast University

Jian Ge
Southeast University

Guang Cheng
Southeast University

Abstract

The network flow watermarking technique associates the two communicating parties by actively modifying certain characteristics of the stream generated by the sender so that it covertly carries some special marking information. Some curious users communicating with the hidden server as a Tor client may attempt de-anonymization attacks to uncover the real identity of the hidden server by using this technique. This compromises the privacy of the anonymized communication system. Therefore, we propose a defense scheme against flow watermarking. The scheme is based on deep neural networks and utilizes generative adversarial networks to convert the original Inter-Packet Delays (IPD) into new IPDs generated by the model. We also adopt the concept of adversarial attacks to ensure that the detector will produce an incorrect classification when detecting these new IPDs. This approach ensures that these IPDs are considered "clean", effectively covering the potential watermarks. This scheme is effective against time-based flow watermarking techniques.

1 Introduction

Traffic analysis is a technique for inferring sensitive information from network traffic patterns, particularly packet timing and size, rather than packet content. Because encryption does not significantly alter traffic patterns, traffic analysis is primarily used in scenarios where network traffic is encrypted, particularly in the dark web. Traditional traffic analysis, including website fingerprinting attacks [21, 29, 30] and flow correlation attacks [8, 18, 20], primarily relies on passive analysis methods. These methods require the collection of a significant amount of traffic data at key location nodes in the network, which involves analyzing various traffic features to confirm the relationship between each network flow. Hence, these processes demand substantial storage space and computational resources, making it less scalable. As a result, active network flow watermarking technology has emerged.

Network Flow Watermarking (NFW) technology is primarily based on the concept of digital watermarking [1]. NFW

covertly embeds special marking information, known as watermarks, into network flows by actively modifying certain characteristics of the flows generated by the sender. After transmission through the communication network, if the receiver can detect the corresponding watermark from the network flow, it is considered that there is a network flow correlation between the sender and the receiver, and thus an explicit communication relationship between them can be recognized. This technique offers the advantages of reduced space-time overhead and high scalability. With the help of this technique, some curious users (e.g., a law enforcement agency) can perform de-anonymization attacks to uncover the real identity of the hidden server while communicating with it as a Tor client, thereby compromising the privacy of the anonymous communication system.

In fact, after years of research, flow watermarking has a trend of evolving towards flow fingerprinting [10], which has the ability to embed more bits of information. Numerous innovative schemes have been proposed. Through the use of various side channels, these schemes achieve the dual effect of invisibility and robustness in attacks. Recently, with the advancement of Deep Neural Network (DNN) technology, the first flow fingerprinting scheme using DNN was proposed in the literature [27]. This scheme significantly enhances the performance of flow fingerprinting and intensifies the threat to the privacy of anonymous communication systems (e.g., Tor). Therefore, there is an urgent need for an effective defense strategy, particularly against flow fingerprinting using DNNs.

Currently, the proposed schemes focus on detecting the presence of watermarks. For example, Peng et al. [25] stated that the Kolmogorov-Smirnov (K-S) test can effectively detect watermarking techniques based on the Inter-Packet Delay (IPD). Jia et al. [13] proposed an MSAC attack method to detect the presence of DSSS watermarks. Defense against watermarking does not seem to receive much attention.

Therefore, we propose a DNN-based defense scheme against flow watermarking for the first time. This scheme utilizes Generative Adversarial Networks (GAN) [6] to convert the original Inter-Packet Delays (IPDs) into new IPDs

generated by the model. We also draw inspiration from adversarial attacks [31], ensuring that the detector will produce an incorrect classification when detecting these new IPDs. This approach guarantees that these IPDs are "clean" and cover the potential watermarks. This scheme can effectively resist time-based flow watermarking techniques. The main contributions of this paper are as follows:

- (1) We propose a flow watermarking defense scheme named DeMarking which is based on adversarial attacks and GANs. The scheme can be utilized in the Tor network to enhance anonymity and provides a strong defense against time-based watermarking.
- (2) We observe through extensive experiments that the small perturbations used in adversarial attacks in the image domain are unnecessary in the watermarking domain. From a defense standpoint, IPDs do not need to remain somewhat similar before and after the perturbation. Based on this property, we replace potentially watermarked IPDs with clean IPDs generated by the model, which significantly enhances the defense effect.
- (3) We design a remapping function to control the range of the mean and standard deviation of the generated IPDs, thereby reducing the impact on the traffic rate and the performance of Tor. Additionally, we employ cosine similarity to transform the gradient boosting, commonly used in adversarial attacks, into gradient descent to facilitate the solution.
- (4) We also experiment with conventional flow watermarking schemes that do not utilize deep neural networks. Our scheme also offers strong protection against conventional flow watermarking methods, such as RAINBOW [11] and SWIRL [9].

The rest of this paper is organized as follows. In Section 2, we investigate the carrier of flow watermarking. In Section 3, we introduce the scenario of this paper. Sections 4 and 5 present some preliminaries and outline the scheme of this paper. Sections 6 and 7 illustrate the experimental setups and results. Finally, we discuss the limitations and future directions of our scheme in Section 8 and conclude the paper in Section 9.

2 Related Works

Since the concept of NFW was first proposed in 2001 [34], researchers have explored numerous carriers for embedding watermarks, including content, timing, size, and rate. The timing-based carriers can be further subdivided into: IPD, Interval Centroid, and Interval Packet Counting. Encrypted communication has become mainstream due to the widespread use of SSL/TLS protocols. Content-based and size-based watermarking have gradually faded out of the researchers' focus

Table 1: Watermarking schemes and carriers.

Watermarking Schemes	Diversities	Carriers
Wang et al. [34]	-	Content
Wang et al. [33]	Time	IPD
Wang et al. [32]	Time	Centroid
Yu et al. [35]	Frequency	Rate
Pyun et al. [26]	Time	Counting
Houmansadr et al. [11]	Time	IPD
Houmansadr et al. [9]	Time	Centroid
Ling et al. [15]	Time	Size
Iacovazzi et al. [12]	Time	IPD
Rezaei et al. [27]	Time	IPD

due to their unsuitability for encrypted traffic. Timing-based watermarking is widely welcomed by researchers due to its better retention in network transmission. This is the reason why there are many subcategories of timing-based carriers.

From the perspective of traditional telecommunications systems, all these carriers ultimately fall into three diversity schemes: time diversity, frequency diversity, and space diversity. Table 1 presents a collection of watermarking schemes and their corresponding carriers.

Through our investigation, we find that timing plays a significant role in watermarking carriers. Even when certain watermarking schemes do not explicitly use timing as a carrier, they are still influenced to some extent by time. For instance, when using rate as a carrier, we can modify IPDs to change the transmission rate of the traffic.

Therefore, our scheme focuses on time-based watermarking as the primary adversary. We leverage the concepts of GANs and adversarial attacks to transform the original IPDs in the network transmission into clean IPDs generated by a model. This enables us to defend against time-based watermarking effectively.

3 Scenario

An anonymous communication system refers to a communication system that employs techniques such as data forwarding, content encryption, and traffic obfuscation on existing networks to conceal communication content and relationships. Among them, Tor is one of the most widely used anonymous communication systems. Our scenario is under the Tor network, which can be generally categorized into three-hop and six-hop according to whether it adopts the hidden service technique or not. Our proposed defense scheme, DeMarking, can be adapted to both scenarios. In this paper, we choose the more challenging six-hop scenario to prove the efficiency of DeMarking.

The core idea of Tor is to provide protection for users' communication privacy through multi-hop proxies and layered encryption. When a Tor Hidden Server (HS) is launched, it

selects three Tor nodes as its entry proxies. Similarly, when a client accesses the HS, it also establishes three proxies to conceal its identity. After the initial configuration is completed, the client selects a rendezvous point (RPO) as the convergence point for communication between the client and the HS. Both the client and the HS establish links to the rendezvous point, completing the construction of the 6-hop circuit, and communication can begin. Tor users access hidden servers through a six-hop circuit, during which no single node can simultaneously know the Tor client’s IP address, the hidden server’s IP address, and the data content. This ensures the anonymity of the Tor client and the hidden server. The aforementioned process is illustrated in Figure 1.

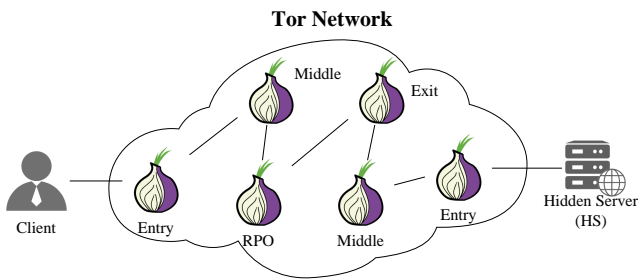


Figure 1: Tor network topology.

Network watermarking technology comprises two main components: the watermarker and the watermark detector. The positions of these two components are designed and selected based on the desired objectives and the expected observation points of the target traffic. In the Tor network scenario depicted in Figure 1, the watermarker is typically located near the client to facilitate embedding, while the watermark detector is generally positioned closer to the HS to determine its true identity. The watermarker is responsible for converting watermark bits or fingerprint information into watermark codes with specific characteristics and embedding them into the target flow. On the other hand, the watermark detector monitors network traffic passing through specific nodes, analyzes traffic features to detect watermarked flows, and subsequently decodes the watermark to extract the embedded information.

To defend against flow watermarking, the transformation of IPD must occur after watermark embedding and before extraction. As depicted in Figure 2, the watermarker is located between the client and its entry node, while the watermark detector is positioned between the HS and the entry node. In this scenario, we can choose one or more of the six proxy nodes between the client and the HS to deploy defense mechanisms. For simplicity, we select only the entry node of the HS as the Tor node with defense.

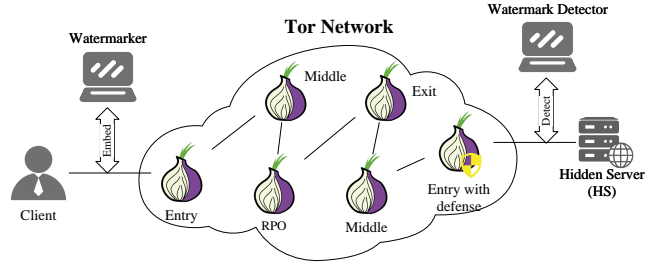


Figure 2: Flow watermarking and its defense.

4 Preliminaries

In this section, we introduce conventional watermarking techniques and DNN-based watermarking techniques. Furthermore, we introduce adversarial attacks and migrate them to the watermarking domain, laying the groundwork for our defense scheme.

4.1 Flow Watermarking Techniques

As stated in Section 2, time is a popular watermarking carrier. Therefore, we select two state-of-the-art watermarking schemes based on different time carriers to introduce.

RAINBOW: Houmansadr et al. [11] proposed the RAINBOW watermarking scheme, which is a non-blind watermarking scheme based on IPD. In this scheme, the watermarker records the timestamps of the passed packets and stores them in a database that is shared with the watermark detector. Additionally, the watermarker introduces a certain delay in the IPD, which is also shared with the watermark detector. When the traffic reaches the watermark detector, it records the timestamps of the packets. By combining the IPD records in the database and calculating the normalized correlation, the watermark detector can ascertain whether the flow has been marked.

SWIRL: The SWIRL watermarking scheme, also proposed by Houmansadr et al. [9], is based on interval centroids. This scheme divides the time into a base interval and a mark interval. The packets within the base interval are used to calculate the interval centroid, which represents the average distance of the packets from the start of the interval. By quantizing the interval centroid, the scheme determines the embedding mode used in the mark interval. The mark interval is further subdivided into multiple sub-intervals, each of which is divided into several time slots. The goal of embedding is to ensure that only the designated time slots contain packets in each sub-interval, which can be achieved by introducing delays in the packets. To detect the presence of a watermark, the detector also calculates the interval centroid based on the base interval. Then, it measures the proportion of packets in the mark interval that fall into the correct time slots. If this proportion exceeds a specific threshold, the watermark is

detected.

Our defense scheme provides good defense against time-based watermarking. In Section 7, we will conduct an experimental analysis specifically targeting these two watermarking schemes.

4.2 DNN-based Watermarking

DNN-based watermarking techniques often employ autoencoder architectures. Autoencoders were initially proposed by Rumelhart et al. [28] and have been widely applied in the field of image watermarking [3–5, 14, 16]. Recently, Rezaei et al. [27] applied autoencoders to the design of flow fingerprinting schemes, using IPD as the watermark carrier to enhance the performance of flow fingerprinting. The architecture of DNN-based flow watermarking is illustrated in Figure 3.

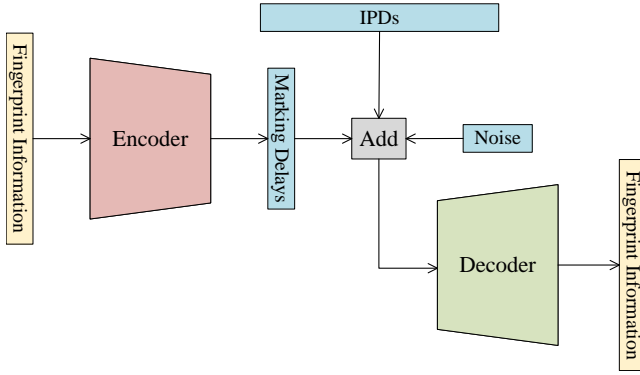


Figure 3: The architecture of DNN-based flow watermarking.

As depicted in the figure, the input of the Encoder is a one-hot vector of length m , representing the fingerprint information to be embedded. The output is a watermark delay vector of length n . Here, m and n are hyperparameters. To embed the watermark, the watermark delay vector is added to a segment of IPD with the same length of n . Due to the inherent delays and jitter introduced during network transmission, some noise is typically added to enhance the robustness of the model. The input of the Decoder is the IPD with watermark delays and noise, which has the same length as the output of the Encoder. The objective of the Decoder is to reconstruct the embedded fingerprint information, which is the same as the input of the Encoder. The trained Encoder and Decoder are then deployed as the watermarker and watermark detector, respectively, in the target network.

4.3 Adversarial Attacks

Adversarial attacks generally mislead the model to make incorrect classifications or predictions by adding subtle perturbations to the model inputs. Such inputs to which subtle perturbations are added are called adversarial samples. The

generation of the adversarial sample \mathbf{x}^* can be formulated as the following optimization problem:

$$\mathbf{x}^* = \mathbf{x} + \arg \min_{\delta} \forall \mathbf{x} \in D_x : O(\mathbf{x} + \delta) \neq O(\mathbf{x}), \quad (1)$$

where \mathbf{x} is the non-adversarial sample, δ is the added adversarial perturbation, D_x represents the set of possible inputs, and $O(\cdot)$ denotes the output of the target model or classifier. Since the target model $O(\cdot)$ is a deep neural network, it is not possible to find a closed-form solution to this optimization problem. Therefore, the equation can be numerically solved using empirical approximation techniques.

$$\arg \max_{\delta} \mathbb{E}_{\mathbf{x} \in D_x} [L(O(\mathbf{x} + \delta), O(\mathbf{x}))], \quad (2)$$

where $L(\cdot)$ is the loss function used to measure the distance between the outputs of the target model before and after the perturbation.

The objective of an adversary is to add the minimal perturbation δ to force the target model to make incorrect classifications. Adversarial samples are commonly studied in image classification applications. One constraint in finding adversarial samples is that the added noise should be imperceptible to the human eye to ensure that the image does not undergo significant changes.

Previous work [19] seemed to make this assumption when perturbing the IPD. It ensured that there would be no significant changes in the IPD before and after perturbation. However, when it comes to network communication, we are not concerned about the exact shape of the IPD. Our main concern is to ensure that it does not have a significant impact on the transmission rate. Under this condition, we can completely use an IPD sequence \mathbf{y} that has a similar mean and standard deviation to \mathbf{x} but is entirely different from it.

To achieve this, we propose a converter model C . When provided with the original IPD sequence \mathbf{x} , the converter transforms it into a new IPD sequence $\mathbf{y} = C(\mathbf{x})$. Therefore, our optimization objective becomes optimizing the parameters of the converter model C . Thus, equation 2 can be adjusted as follows:

$$\arg \max_C \mathbb{E}_{\mathbf{x} \in D_x} [L(O(C(\mathbf{x})), O(\mathbf{x}))]. \quad (3)$$

4.4 Cosine Similarity

Previous works [2, 7, 17] have utilized gradient boosting to maximize the loss of the target model in adversarial attacks. To enhance implementation efficiency, we employ cosine similarity as the distance metric, which transforms the gradient boosting into gradient descent. The formula for calculating cosine similarity is as follows:

$$\cos(\mathbf{a}, \mathbf{b}) = \frac{\mathbf{a} \cdot \mathbf{b}}{|\mathbf{a}| \cdot |\mathbf{b}|} = \frac{\sum_{i=1}^n a_i b_i}{\sqrt{\sum_{i=1}^n a_i^2} \cdot \sqrt{\sum_{i=1}^n b_i^2}}. \quad (4)$$

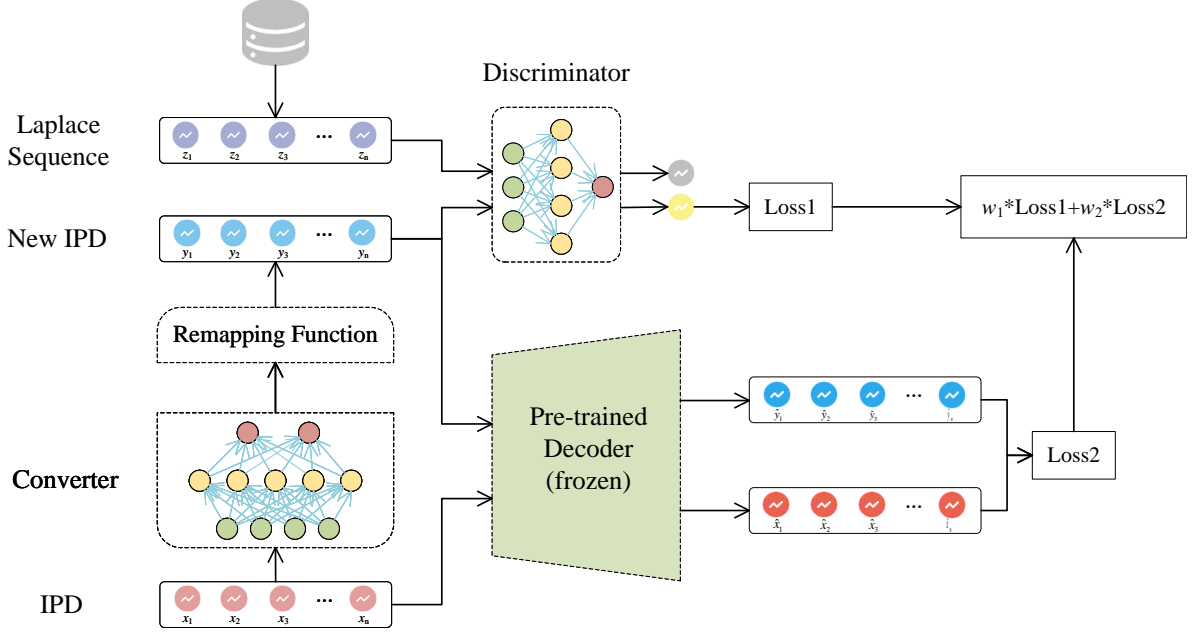


Figure 4: Training architecture.

The cosine similarity is a value between -1 and 1. When vectors \mathbf{a} and \mathbf{b} are more similar, $\cos(\mathbf{a}, \mathbf{b})$ approaches 1, and conversely, it approaches -1. Therefore, the equation 3 can be finally expressed as follows:

$$\arg \min_C \mathbb{E}_{\mathbf{x} \in D_x} [\cos(O(C(\mathbf{x})), O(\mathbf{x}))]. \quad (5)$$

5 Design of DeMarking

Since the IPD sequence should adhere to the expected statistical distribution of the target protocol, we design a discriminator based on the concept of GAN to guide the generation of IPDs by the converter. In conjunction with the adversarial attack discussed in Section 4.3, we design the following architecture to train the converter to generate IPD sequences that meet the desired criteria, as shown in Figure 4.

Converter: The converter is a fully connected network whose parameters are learned during training. Its input is an IPD sequence $\mathbf{x} = \{x_1, x_2, \dots, x_n\}$ of length n . The output is a new IPD sequence $\mathbf{y} = \{y_1, y_2, \dots, y_n\}$ of the same length, obtained after passing through a remapping function. This new IPD sequence \mathbf{y} will be clean and will replace the original IPD to implement the defense mechanism.

Discriminator: The discriminator is also a fully connected network. It is responsible for distinguishing between the data generated by the converter and the data from the target distribution (e.g., Laplace distribution), guiding the converter to generate data that conforms to a specific distribution. The input of the discriminator, similar to the converter, is a vector of length n . The output of the discriminator is transformed

into a probability value through the sigmoid function.

Decoder: The decoder is a pre-trained model discussed in Section 4.2, and its parameters are frozen. Under the white-box condition, it has the same structure and parameters as the adversary’s decoder. Under the black-box condition, it is a custom structure trained as described in Section 4.2. The decoder extracts the embedded fingerprint information of length m from the IPD sequences of length n . In the figure 4, \mathbf{x} and \mathbf{y} are input to the decoder, and $\hat{\mathbf{x}}$ and $\hat{\mathbf{y}}$ are obtained as outputs.

Since we employ a generative adversarial network, we have two loss functions to control the performance of each task: the discriminator loss and the converter loss. For the discriminator, we utilize the Mean Absolute Error (MAE) to evaluate its discrimination effectiveness. As for the converter, we aim to generate data that conforms to a specific distribution while also misleading the decoder through adversarial attacks. To balance these objectives, we introduce two weights, w_1 and w_2 , resulting in $w_1 * Loss1 + w_2 * Loss2$ as depicted in the figure 4. Here, $Loss1$ represents the scores provided by the discriminator, and $Loss2$ measures the distance between the extracted vectors using the cosine similarity described in Section 4.4.

Table 2 provides a detailed overview of the structures of the converter and the discriminator. The Adam optimizer is employed for training in both cases.

In addition to ensuring that the IPD sequence conforms to a specific distribution, it is also important to minimize the introduction of excessive delay during defense, as this can interfere with the underlying application. Therefore, we design a remapping function $R(\cdot)$ to control the value of the

Table 2: Details of the model structure.

	Layer	Details
Converter	Fully Connected 1	Size: 1024, Activation: LeakyRelu
	Fully Connected 2	Size: 2048, Activation: LeakyRelu
	Fully Connected 3	Size: 512, Activation: LeakyRelu
Discriminator	Fully Connected 1	Size: 2048, Activation: Relu

generated IPD sequence. The specific details are as follows:

$$R(C(\mathbf{x}), \mu_{\min}, \mu_{\max}, \sigma) = C(\mathbf{x}) * \frac{\min(\text{std}(C(\mathbf{x})), \sigma)}{\text{std}(C(\mathbf{x}))} - \max\left(\overline{C(\mathbf{x})} - \mu_{\max}, 0\right) - \min\left(\overline{C(\mathbf{x})} - \mu_{\min}, 0\right), \quad (6)$$

where $\overline{C(\mathbf{x})}$ represents the mean of the generated new IPD sequence $C(\mathbf{x})$, μ_{\min} and μ_{\max} are the lower and upper bounds, respectively, that we aim to restrict the range of $\overline{C(\mathbf{x})}$, and σ is the maximum allowable standard deviation. By utilizing this remapping function, we can control the mean of the newly generated IPD sequence within a specific range.

To apply the trained converter to real-time network traffic, we design Algorithm 1. During the defense initiation, a random sequence of length n , $\mathbf{x}_0 = \{x_{0,1}, x_{0,2}, \dots, x_{0,n}\}$, is generated. \mathbf{x}_0 is then fed into the converter and passed through the remapping function, resulting in a new IPD sequence, $\mathbf{y}_0 = \{y_{0,1}, y_{0,2}, \dots, y_{0,n}\}$. When network packets arrive, their timestamps, $\mathbf{t}_0 = \{t_0, t_1, \dots, t_n\}$, are recorded, and the IPD is replaced with \mathbf{y}_0 . Once \mathbf{y}_0 is exhausted, $\mathbf{x}_1 = \{t_1 - t_0, t_2 - t_1, \dots, t_n - t_{n-1}\}$ is computed based on the timestamps \mathbf{t}_0 . The subsequent defense process is repeated following the aforementioned steps.

6 Experimental Setup

In this section, we discuss our experimental setup. All our code was written in Python, and the DNN techniques were implemented using PyTorch [24].

6.1 Metrics

Flow watermarking and flow fingerprinting techniques differ in terms of the number of embedded bits. Watermarking techniques only consider embedding a single watermark bit, while flow fingerprinting embedding consists of multiple bits representing fingerprint information. Therefore, for these two techniques, we employ different evaluation metrics.

For watermarking techniques, we employ the True Positive (TP) and False Positive (FP) rates as evaluation metrics.

- TP: The ratio of flows correctly identified as containing watermarks and actually embedded with watermarks, to the total number of flows with watermarks.
- FP: The ratio of flows incorrectly identified as containing watermarks but not actually embedded with watermarks, to the total number of flows without watermarks.

Algorithm 1: DeMarking defense scheme

Data :

$n \leftarrow$ the length of the IPD sequence

$\mathbf{q} \leftarrow$ the packet buffer queue

$\mathbf{t} \leftarrow$ the packet timestamp buffer queue

$\mu_{\min} \leftarrow$ lower bound on the mean value of the generated IPDs

$\mu_{\max} \leftarrow$ upper bound on the mean of the generated IPDs

$\sigma \leftarrow$ upper bound on the standard deviation of the generated IPDs

$\mathbf{x} = \{x_{0,1}, x_{0,2}, \dots, x_{0,n}\} \leftarrow$ randomly initialized IPDs

$\mathbf{y} = R(C(\mathbf{x}), \mu_{\min}, \mu_{\max}, \sigma) \leftarrow$ Convert \mathbf{x} to obtain new IPDs

Thread 1:

1 **while** a packet arrives :

2 | put the packet into \mathbf{q}

3 | record the timestamp into \mathbf{t}

Thread 2:

1 **while** true :

2 | **while** \mathbf{y} is not empty :

3 | | sleep(y_0) and remove y_0 from \mathbf{y}

4 | | **if** \mathbf{q} is not empty :

5 | | | send packet q_0 and remove q_0 from \mathbf{q}

6 | | **else:**

7 | | | send a random packet

8 | | $l = \min(n, \text{len}(\mathbf{t}))$

9 | | **for** $i \in \{1, 2, \dots, l\}$:

10 | | | $x_i = t_i - t_{i-1}$

11 | | **if** $l < n$:

12 | | | **for** $i \in \{l+1, \dots, n\}$:

13 | | | | $x_i =$ a random IPD

14 | | remove t_0, t_1, \dots, t_l from \mathbf{t}

15 | | $\mathbf{y} = R(C(\mathbf{x}), \mu_{\min}, \mu_{\max}, \sigma)$

For flow fingerprinting techniques, we utilize the Extraction Rate (ER) and Bit Error Rate (BER) as evaluation metrics.

- ER: The ratio of the number of flows from which the fingerprint can be successfully extracted to the total number of flows with fingerprints.
- BER: We convert each fingerprint to its binary representation to calculate the BER. It is important to note that we

Table 3: Details of the adversary model.

	Layer	Details
Encoder	Fully Connected 1	Size: 1000, Activation: Relu
	Fully Connected 2	Size: 2000, Activation: Relu
	Fully Connected 3	Size: 2000, Activation: Relu
	Fully Connected 4	Size: 500, Activation: Relu
Decoder	Convolution Layer 1	Kernel number: 50
		Kernel size: 10
		Stride: (1,1)
		Activation: Relu
Decoder	Convolution Layer 2	Kernel number: 10
		Kernel size: 10
		Stride: (1,1)
		Activation: Relu
	Fully Connected 1	Size: 128, Activation: Relu

consider the average bit error rate across all fingerprints.

6.2 Adversary Setup and Models

We assume that the flow fingerprinting adversary adopts the model structure described in reference [27] and utilizes the Adam optimizer. The specific details are shown in Table 3.

In the white-box scenario, we can directly utilize the known model and its parameters. However, in the black-box scenario, we lack knowledge about the adversary’s model, parameters, or dataset. Therefore, we leverage the transferability of adversarial attacks [22, 23] to design a custom substitute model. Based on this substitute model, we train a converter to defend against the adversary’s model.

In order to demonstrate the effectiveness of our approach against traditional watermarking techniques as well, we reproduce RAINBOW [11] and SWIRL [9] using Python. We conduct experiments on these techniques using the trained converter.

6.3 Datasets

To obtain real-world traffic data, we set up a traffic collection environment based on the scenario described in Section 3. We use two Alibaba Cloud servers running Ubuntu 20.04, with Tor version 0.4.2.7 installed. One server is located in Hong Kong, serving as the client, while the other server is located in Singapore, serving as the HS. The client accesses the HS through six real-world Tor nodes. Since watermarking techniques only consider the one-way link from the client to the HS, we generate traffic by uploading a randomly generated 3MB file. We divide the experiments into two groups, with each group performing 500 uploads to obtain datasets D_1 and D_2 , respectively. Due to the automatic circuit switching feature of Tor, our data is not always collected on the same circuit. Based on the source IP, destination IP, and protocol

type, we can easily distinguish the target flows and extract the packet timestamps for calculating IPD.

7 Experimental Results

To demonstrate the effectiveness of our scheme, we first conduct defense experiments on the adversary model described in Section 6.2 under both white-box and black-box conditions. Subsequently, we perform defense experiments on RAINBOW and SWIRL using the trained converter. Finally, we evaluate the computational cost of our approach.

7.1 White Box

Assuming that we want to embed fingerprint information of 10 bits, the input to the Encoder is a one-hot vector of length 1024. For the output of the Encoder, we select four different output lengths: 50, 100, 150, and 200, corresponding to four different model sizes. We set the remapping function to control the mean of the generated IPDs between 30 and 60, with a standard deviation of less than 20. We use dataset D_1 , with 80% of the data used for training and 20% for testing.

First, we train the adversary model on the training set until convergence. Then, we use the IPD sequences with watermarking delays generated by the adversary model as input to the Converter and train it based on the training architecture shown in Figure 4.

We measure the extraction rate and bit error rate of the model with and without defense. The results are shown in Table 4.

From Table 4, we can observe that our defense scheme is highly effective. Without defense, the adversary model can successfully extract the fingerprint information with extraction rates of over 95% and low bit error rates. However, with defense, the extraction rate of the adversary model is nearly zero, and the bit error rate increases to 50%. This

Table 4: ER and BER with and without defense in white-box scenarios.

Length of IPD sequences	ER		BER	
	Without defense(%)	With defense(%)	Without defense(%)	With defense(%)
50	99.307	0.098	0.316	50
100	97.542	0.098	1.290	50
150	99.211	0.098	0.403	50
200	98.809	0.098	0.587	50

Table 5: Details of the substitute model.

	Layer	Details
Encoder	Fully Connected 1	Size: 500, Activation: Relu
	Fully Connected 2	Size: 2000, Activation: Relu
Decoder	Fully Connected 1	Size: 1000, Activation: Relu
	Fully Connected 2	Size: 3000, Activation: Relu

aligns with our calculated expectation: given a bit sequence of length l , randomly generating another bit sequence of the same length, we can compute the expected bit error rate as $\frac{1 * C_l^1 + 2 * C_l^2 + \dots + l * C_l^l}{2^{l * l}} = 0.5$.

7.2 Black Box

In the black-box scenario, we assume that the adversary uses a model with an output length of 100, as described in Section 7.1. Since we do not have access to the details of the adversary’s model or the dataset they use, we first establish a substitute model with an input length of 1024. The details of the substitute model are shown in Table 5.

It can be observed that our substitute model is simple yet effective. We also select output lengths of 50, 100, 150, and 200 for the substitute model. To differentiate it from the adversary’s dataset, we train the substitute models of different sizes on the dataset D_2 until convergence. Based on these substitute models and the training architecture shown in Figure 4, we train the corresponding Converters. It is important to note that the training of the Converters is also conducted on dataset D_2 .

After the training is completed, we perform defense experiments against the adversary model on the dataset D_1 using Converters with lengths of 50, 100, 150, and 200, respectively. Dataset D_1 is the dataset used by the adversary model. The defense results are presented in Table 6.

Table 6: ER and BER with defense in black-box scenarios.

Length of IPD sequences	ER(%)	BER(%)
50	0.033	49.997
100	0.167	49.833
150	0.133	50.407
200	0.133	49.620

It is evident that without defense, the extraction rate and bit error rate of the adversary model are 97.542% and 1.290%

respectively, as shown in Table 4. After applying defense in the black-box scenario, the extraction rate is nearly reduced to zero, and the bit error rate increases to around 50%, as shown in Table 6. Therefore, our defense scheme demonstrates effective results in both white-box and black-box scenarios.

Unlike conventional schemes that just add perturbations to IPDs, our scheme involves a comprehensive transformation of IPDs. The magnitude of the changes introduced is significantly higher compared to perturbations, leading to alterations in IPD patterns. Consequently, after the defense, it becomes challenging for the Decoder to extract the fingerprint information.

7.3 Conventional Watermarking Techniques

In order to demonstrate the effectiveness of our defense against conventional watermarking techniques, we conduct experiments on RAINBOW and SWIRL using the four Converters trained in the black-box scenario. The experiments are conducted using the dataset D_1 , which differs from the dataset D_2 used for training the models.

RAINBOW: We use the first 1200 IPDs of each flow in the dataset D_1 for watermark embedding. The watermark perturbation amplitude is set to 10, and the detection threshold for the watermark is set to 0.54. These parameter values are recommended in the literature. During the experiments, we simulate network jitter using a Laplace distribution with a location parameter of 0 and a scale parameter of 10. The changes in the TP rate with and without defense are shown in Figure 5.

It can be observed that after applying our defense, the TP rate of RAINBOW is always reduced to zero regardless of the flow length, which shows the robustness of the DeMarking. We also observe that the FP rate is close to zero regardless of whether the defense is applied or not, so we do not list it.

SWIRL: SWIRL is based on interval centroids and is more complex than RAINBOW. The parameters for SWIRL are

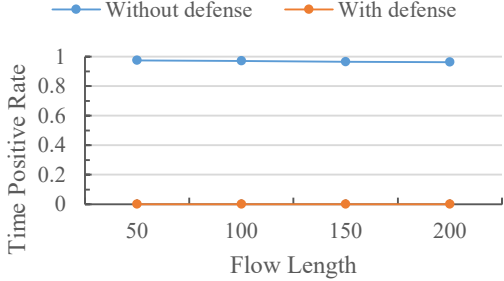


Figure 5: Experimental results of RAINBOW.

also set to the recommended values found in the literature. The interval length is set to 2 seconds, with 20 subintervals and 5 slots. The packet detection threshold is set to 0.5, and the mark detection threshold is set to 12 out of 32 interval pairs. In the absence of defense, our experiments show that SWIRL achieves a TP rate of 96.689%. However, after applying our defense, regardless of which Converter is used, the TP rate is reduced to 0%. Similar to RAINBOW, the FP rate is nearly zero regardless of the presence or absence of defense.

7.4 Computational Costs

Since the defense of watermarking needs to be performed in real-time over network transmissions, the computational cost of the defense components is an important metric for evaluating the feasibility of the defense. The GPU we use is GeForce RTX 3090. To evaluate the computational cost, we measure the conversion elapsed time of one IPD record as an indicator. We use one IPD record as the input to the Converter and calculate the average time over 10,000 iterations. The measured conversion time is shown in Figure 6.

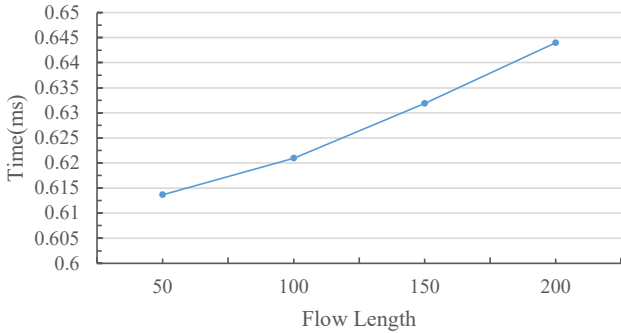


Figure 6: Computational costs of converters.

It can be observed that the conversion time for a single IPD sequence is approximately 0.6 milliseconds, which is negligible for IPDs. Therefore, our defense approach is capable of handling real-time network transmissions.

8 Limitations and Future Directions

As previously mentioned, this work focuses on defending against time-based watermarking. Our study shows that our proposed defense scheme achieves good results against flow fingerprinting [27] based on DNN and some conventional watermarking techniques [9, 11]. To accomplish this, we incorporate techniques such as GANs and adversarial attacks.

However, it is important to emphasize that our defense scheme is only applicable to watermarking schemes influenced by IPDs. For other types of watermarks based on content, size, rate, and other carriers, our defense method may not be applicable. Therefore, in future research, we encourage the inclusion of a wider range of watermark carriers within our defense framework to enhance the defense capabilities against various types of watermarking techniques.

It should be noted that the inclusion of these watermark carriers may require further research and exploration. We believe that by continuously improving and expanding the defense against watermarking, we can provide more effective protection for our communication privacy.

9 Conclusions

In this paper, we introduce a defense scheme against time-based watermarking which can be called DeMarking. DeMarking utilizes techniques such as GAN and adversarial attacks to transform the original IPD sequence into a new, clean IPD sequence, thereby achieving defense. We also construct a remapping function to minimize the impact on network flows.

We evaluate our defense against DNN-based flow fingerprinting techniques. Even in the black-box scenario, our defense demonstrates good effectiveness. We also evaluate our defense against conventional watermarking techniques, including different time carriers, and achieve satisfactory defense results. Finally, we measure the computational cost of our scheme. The computational time required for our defense is negligible compared to an IPD, allowing it to handle real-time network transmissions.

References

- [1] Ingemar Cox, Matthew Miller, Jeffrey Bloom, and Chris Honsinger. Digital watermarking. *Journal of Electronic Imaging*, 11(3):414–414, 2002.
- [2] Yinpeng Dong, Fangzhou Liao, Tianyu Pang, Hang Su, Jun Zhu, Xiaolin Hu, and Jianguo Li. Boosting adversarial attacks with momentum. In *Proceedings of the IEEE conference on computer vision and pattern recognition*, pages 9185–9193, 2018.
- [3] Han Fang, Kejiang Chen, Yupeng Qiu, Jiayang Liu, Ke Xu, Chengfang Fang, Weiming Zhang, and Ee-Chien

- Chang. Denol: A few-shot-sample-based decoupling noise layer for cross-channel watermarking robustness. In *Proceedings of the 31st ACM International Conference on Multimedia*, pages 7345–7353, 2023.
- [4] Han Fang, Zhaoyang Jia, Zehua Ma, Ee-Chien Chang, and Weiming Zhang. Pimog: An effective screen-shooting noise-layer simulation for deep-learning-based watermarking network. In *Proceedings of the 30th ACM International Conference on Multimedia*, pages 2267–2275, 2022.
- [5] Jiayun Fu, Bin B Zhu, Haidong Zhang, Yayi Zou, Song Ge, Weiwei Cui, Yun Wang, Dongmei Zhang, Xiaojing Ma, and Hai Jin. Chartstamp: Robust chart embedding for real-world applications. In *Proceedings of the 30th ACM International Conference on Multimedia*, pages 2786–2795, 2022.
- [6] Ian Goodfellow, Jean Pouget-Abadie, Mehdi Mirza, Bing Xu, David Warde-Farley, Sherjil Ozair, Aaron Courville, and Yoshua Bengio. Generative adversarial nets. *Advances in neural information processing systems*, 27, 2014.
- [7] Ian J Goodfellow, Jonathon Shlens, and Christian Szegedy. Explaining and harnessing adversarial examples. *arXiv preprint arXiv:1412.6572*, 2014.
- [8] Zhong Guan, Chang Liu, Gang Xiong, Zhen Li, and Gaopeng Gou. Flowtracker: Improved flow correlation attacks with denoising and contrastive learning. *Computers & Security*, 125:103018, 2023.
- [9] Amir Houmansadr and Nikita Borisov. Swirl: A scalable watermark to detect correlated network flows. In *NDSS*. Citeseer, 2011.
- [10] Amir Houmansadr and Nikita Borisov. The need for flow fingerprints to link correlated network flows. In *Privacy Enhancing Technologies: 13th International Symposium, PETS 2013, Bloomington, IN, USA, July 10-12, 2013. Proceedings 13*, pages 205–224. Springer, 2013.
- [11] Amir Houmansadr, Negar Kiyavash, and Nikita Borisov. Rainbow: A robust and invisible non-blind watermark for network flows. In *NDSS*, volume 47, pages 406–422. Citeseer, 2009.
- [12] Alfonso Iacovazzi, Sanat Sarda, Daniel Frassinelli, and Yuval Elovici. Dropwat: An invisible network flow watermark for data exfiltration traceback. *IEEE Transactions on Information Forensics and Security*, 13(5):1139–1154, 2017.
- [13] Weijia Jia, Fung Po Tso, Zhen Ling, Xinwen Fu, Dong Xuan, and Wei Yu. Blind detection of spread spectrum flow watermarks. In *IEEE INFOCOM 2009*.
- [14] Zhaoyang Jia, Han Fang, and Weiming Zhang. Mbrs: Enhancing robustness of dnn-based watermarking by mini-batch of real and simulated jpeg compression. In *Proceedings of the 29th ACM international conference on multimedia*, pages 41–49, 2021.
- [15] Zhen Ling, Xinwen Fu, Weijia Jia, Wei Yu, Dong Xuan, and Junzhou Luo. Novel packet size-based covert channel attacks against anonymizer. *IEEE Transactions on Computers*, 62(12):2411–2426, 2012.
- [16] Yang Liu, Mengxi Guo, Jian Zhang, Yuesheng Zhu, and Xiaodong Xie. A novel two-stage separable deep learning framework for practical blind watermarking. In *Proceedings of the 27th ACM International conference on multimedia*, pages 1509–1517, 2019.
- [17] Seyed-Mohsen Moosavi-Dezfooli, Alhussein Fawzi, Omar Fawzi, and Pascal Frossard. Universal adversarial perturbations. In *Proceedings of the IEEE conference on computer vision and pattern recognition*, pages 1765–1773, 2017.
- [18] Milad Nasr, Alireza Bahramali, and Amir Houmansadr. Deepcorr: Strong flow correlation attacks on tor using deep learning. In *Proceedings of the 2018 ACM SIGSAC Conference on Computer and Communications Security*, pages 1962–1976, 2018.
- [19] Milad Nasr, Alireza Bahramali, and Amir Houmansadr. Defeating {DNN-Based} traffic analysis systems in {Real-Time} with blind adversarial perturbations. In *30th USENIX Security Symposium (USENIX Security 21)*, pages 2705–2722, 2021.
- [20] Se Eun Oh, Taiji Yang, Nate Mathews, James K Holland, Mohammad Saidur Rahman, Nicholas Hopper, and Matthew Wright. Deepcoffee: Improved flow correlation attacks on tor via metric learning and amplification. In *2022 IEEE Symposium on Security and Privacy (SP)*, pages 1915–1932. IEEE, 2022.
- [21] Andriy Panchenko, Fabian Lanze, Jan Pennekamp, Thomas Engel, Andreas Zinnen, Martin Henze, and Klaus Wehrle. Website fingerprinting at internet scale. In *NDSS*, 2016.
- [22] Nicolas Papernot, Patrick McDaniel, and Ian Goodfellow. Transferability in machine learning: from phenomena to black-box attacks using adversarial samples. *arXiv preprint arXiv:1605.07277*, 2016.
- [23] Nicolas Papernot, Patrick McDaniel, Ian Goodfellow, Somesh Jha, Z Berkay Celik, and Ananthram Swami. Practical black-box attacks against machine learning. In *Proceedings of the 2017 ACM on Asia conference on computer and communications security*, pages 506–519, 2017.

- [24] Adam Paszke, Sam Gross, Francisco Massa, Adam Lerer, James Bradbury, Gregory Chanan, Trevor Killeen, Zeming Lin, Natalia Gimelshein, Luca Antiga, et al. Pytorch: An imperative style, high-performance deep learning library. *Advances in neural information processing systems*, 32, 2019.
- [25] Pai Peng, Peng Ning, and Douglas S Reeves. On the secrecy of timing-based active watermarking trace-back techniques. In *2006 IEEE Symposium on Security and Privacy (S&P'06)*, pages 15–pp. IEEE, 2006.
- [26] Young June Pyun, Young Hee Park, Xinyuan Wang, Douglas S Reeves, and Peng Ning. Tracing traffic through intermediate hosts that repacketize flows. In *IEEE INFOCOM 2007-26th IEEE International Conference on Computer Communications*, pages 634–642. IEEE, 2007.
- [27] Fatemeh Rezaei and Amir Houmansadr. Finn: fingerprinting network flows using neural networks. In *Annual Computer Security Applications Conference*, pages 1011–1024, 2021.
- [28] David E Rumelhart, Geoffrey E Hinton, and Ronald J Williams. Learning representations by back-propagating errors. *nature*, 323(6088):533–536, 1986.
- [29] Meng Shen, Kexin Ji, Zhenbo Gao, Qi Li, Liehuang Zhu, and Ke Xu. Subverting website fingerprinting defenses with robust traffic representation. In *32nd USENIX Security Symposium (USENIX Security 23)*, pages 607–624, 2023.
- [30] Payap Sirinam, Nate Mathews, Mohammad Saidur Rahman, and Matthew Wright. Triplet fingerprinting: More practical and portable website fingerprinting with n-shot learning. In *Proceedings of the 2019 ACM SIGSAC Conference on Computer and Communications Security*, pages 1131–1148, 2019.
- [31] Christian Szegedy, Wojciech Zaremba, Ilya Sutskever, Joan Bruna, Dumitru Erhan, Ian Goodfellow, and Rob Fergus. Intriguing properties of neural networks. *arXiv preprint arXiv:1312.6199*, 2013.
- [32] Xinyuan Wang, Shiping Chen, and Sushil Jajodia. Network flow watermarking attack on low-latency anonymous communication systems. In *2007 IEEE Symposium on Security and Privacy (SP'07)*, pages 116–130. IEEE, 2007.
- [33] Xinyuan Wang and Douglas S Reeves. Robust correlation of encrypted attack traffic through stepping stones by manipulation of interpacket delays. In *Proceedings of the 10th ACM conference on Computer and communications security*, pages 20–29, 2003.
- [34] Xinyuan Wang, Douglas S Reeves, S Felix Wu, and Jim Yuill. Sleepy watermark tracing: An active network-based intrusion response framework. In *Trusted Information: The New Decade Challenge 16*, pages 369–384. Springer, 2001.
- [35] Wei Yu, Xinwen Fu, Steve Graham, Dong Xuan, and Wei Zhao. Dsss-based flow marking technique for invisible traceback. In *2007 IEEE Symposium on Security and Privacy (SP'07)*, pages 18–32. IEEE, 2007.